ASME 2012 5th Annual Dynamic Systems and Control Conference joint with the JSME 2012 11th Motion and Vibration Conference
DSCC2012-MOVIC2012
October 17-19, 2012, Fort Lauderdale, Florida, USA

DSCC2012-MOVIC2012-8523

OPTIMAL CONTROL OF BUILDING HVAC SYSTEMS IN THE PRESENCE OF IMPERFECT PREDICTIONS

Mehdi Maasoumy*

Department of Mechanical Engineering
University of California
Berkeley, California 94720
Email: mehdi@me.berkeley.edu

Alberto Sangiovanni-Vincentelli

Department of Electrical Engineering
University of California
Berkeley, California 94720
Email: alberto@eecs.berkeley.edu

ABSTRACT

This paper deals with the problem of robust model predictive control of an uncertain linearized model of a building envelope and HVAC system. Uncertainty of the model is due to the *imperfect* predictions of internal and external heat gains of the building. The Open-Loop prediction formulation of the Robust Model Predictive Control (OL-RMPC) is known to be unnecessarily over-conservative in practice. Therefore, we adopt a Closed-Loop prediction formulation of Robust Model Predictive Control (CL-RMPC) which exploits an *uncertainty feedback parameterization* of the control sequence and results in a tractable formulation of the problem. To improve on the efficiency of CL-RMPC we propose a new uncertainty feedback parameterization of the control input, which leads to a number of decision variables *linear* in time horizon as opposed to *quadratic* as in previous approaches. To assess our approach we compare three different robust optimal control strategies: nominal MPC which does not have a priori information of the uncertainty, OL-RMPC and CL-RMPC. We show results from a *quantitative* analysis of performance of these controllers at different prediction error values of the disturbance. Simulations show that CL-RMPC provides a higher level of comfort with respect to OL-RMPC while consuming 36% less energy. Moreover, CL-RMPC maintains perfect comfort level for up to 75% error in the disturbance prediction. Finally, the newly proposed parameterization maintains the performance of CL-RMPC while reducing the simulation time by an average of 30%.

*Address all correspondence to this author.

1 Introduction

Advanced control algorithms are considered critical enablers to achieve low energy consumption in commercial buildings. Entire sections of the ASHRAE 90.1 standard [1] are dedicated to the specification of control requirements. Although the optimal control of an HVAC system is a complex multi-variable problem, it is standard practice to rely on simple control strategies that include PID and bang-bang controllers with hysteresis. In most cases, standard sequences of operations for *typical* installations are used by control contractors. Each sequence controls the HVAC equipment during an operation phase such as optimal start, safety shutdown and normal operation. After installation and tuning, the building is inspected by a commissioning agent that verifies that the building satisfies the owner's expectations. The commissioning agent does not only verify the expected performance right after installation, but also after the building has started its operations.

This short summary of design and validation practices in the building industry shows the importance of a model-based design flow for building controls. To attain energy efficiency, control algorithms need to be tailored to the physical properties of the building at hand rather than being an adaptation of a standard sequence designed for a "typical" building. To design an optimal controller that balances comfort and energy usage, a thermal model of the building is needed. To achieve building-level energy-optimality, the model should be able to capture the interaction between physically connected spaces in the building, occupancy schedules, and state and input constraints.

Optimal control of HVAC components using model-based control techniques has shown promising results for achieving energy efficiency in buildings [2–6]. However, these control tech-

Copyright © 2012 by ASME

niques rely heavily on a perfect (or almost perfect) mathematical model of the building or a perfect estimation of the unmodeled dynamics of the system [2].

Although a great deal of progress has been made in modeling the thermal behavior of building envelope and HVAC system [2, 4, 5, 7–9], the random nature of some components of these systems makes it very hard to predict, with high fidelity, the temperature evolution of the room using mathematical models. These random events and phenomena include building occupancy by people which along with other internal loads such as the heat emitted from electrical devices and lighting, account for the total internal heat generation of the building. The outside environment of the building is also subject to many random and hard-to-accurately-predict phenomena such as the wind speed, solar radiation, cloudiness of the sky and outside air temperature. The aggregate effect of all these factors constitutes the total external heat gain of the building. The authors name these two heat gains of the building, the "unmodeled dynamics" and propose a methodology in [2] to estimate these loads which act as disturbance to the system dynamics. However, as mentioned earlier, it is difficult to obtain a *perfect* prediction of the loads in future times. On the other hand, model-based optimal controllers such as Model Predictive Control (MPC) are highly dependent on accurate predictions of these disturbances. In order to account for these modeling deficiencies, it is usually a reasonable assumption to consider an additive norm-bounded[1] uncertainty to the model. The question here is how to integrate this uncertainty information in the control design to achieve the desired comfort level while consuming *minimum* energy.

We present an overview of existing min-max formulations of Robust Model Predictive Control (RMPC) for uncertain constrained discrete-time systems. A min-max strategy for MPC tries to optimize the worst-case scenario cost function with respect to uncertainties. Standard min-max MPC schemes easily lead to conservative controllers because they typically deal with open-loop formulations. Moreover, Open-Loop Robust Model Predictive Control (OL-RMPC) is known to be unnecessarily overly conservative in most applications [10, 11]. The reason is that the optimal open-loop control sequence has to deal with all the future disturbances without using the information of the future measurements that will be obtained as the horizon window recedes. An extension to min-max MPC that resolves this problem is closed-loop min-max MPC or Closed-Loop Robust Model Predictive Control (CL-RMPC). However, CL-RMPC leads to an intractable problem which is much harder to solve [12]. Fortunately, approximation of closed-loop min-max MPC using a convex programming framework is possible by the use of semidefinite relaxations. The idea in CL-RMPC, is to approximate the intractable min-max problem by introducing new decision variables into the system and parameterize the future control sequence in the future states or disturbances [13, 14].

On the other hand, nominal MPC in practice is regarded as a state feedback controller. The reason is that, although MPC at each time step solves an *open-loop* optimal control problem, only the first entry of the resulting optimal control sequence is implemented on the plant at each time step, and this process is repeated as the prediction horizon recedes. This feedback of the measurement information to the optimization endows the whole procedure with a *robustness*, typical of closed-loop systems [11]. Therefore, nominal MPC is capable of rejecting some level of unmodeled or unpredictable disturbances due to its closed-loop nature.

Note that in the control of building climate, it is not extremely crucial to respect temperature bounds at all times and based on some standards, some level of temperature constraint violations would be acceptable (e.g., the European standards state that the room temperature must be kept within a certain range with a certain probability [3].) and can be tolerated if it translates into considerable reductions in total or peak energy consumption of the whole HVAC system.

Based on the discussion of last three paragraphs, nominal MPC, OL-RMPC, and CL-RMPC, exhibit some level of robustness in their performances. In this paper one of the questions that we will try to answer is: "*which of the above controllers would be the best choice for the building climate control, in the presence of uncertainty*?" We carry out a *quantitative* analysis of the performance of the above controllers. Through simulations we assess the performance of the controllers for a range of prediction accuracies.

A new disturbance feedback parameterization of the input is proposed. It is shown in the paper that this parameterization reduces the number of decision variables of the optimization problem and hence results in a faster alternative than the existing parameterizations in the literature, while maintaining the performance level of the RMPC.

A number of related works can be found in the literature. A model predictive controller was implemented by the authors on the model utilized in this work, in [2]. It was shown that in the case of *perfect* disturbance load prediction the controller manages to maintain the temperature within the comfort zone for all times while reducing the total and peak conditioned air consumption with respect to the existing control strategy of the building, by 68% and 35%, respectively. In [6] the authors investigate a bilinear model under stochastic uncertainty with probabilistic, time varying constraints.

In this work we build upon [2, 8], in which we focused on modeling of the building thermal behavior and concurrent estimation of parameters and unmodeled dynamics. In this paper, we focus on optimal control design in the presence of *imperfect* disturbance predictions. Contribution of this work is twofold:

1. We propose a new disturbance feedback parameterization. Simulations show that the new parameterization enhances the computational and performance characteristics of the CL-RMPC. The new parameterization leads to a number of decision variables, *linear* in time horizon as opposed to *quadratic*, for the previously introduced parameterizations.

[1] Refer to Section 3 for definition and more details.

Copyright © 2012 by ASME

The resulting sparse feedback gain matrix also reduces the simulation time by 30% with respect to the previous parameterization.

2. To validate our approach, we compare the performances of three different controllers for a range of prediction error values. Exhaustive *quantitative* analysis show how much the performance of the MPC will deteriorate in the case of *imperfect* predictions. We quantify how much the energy consumption and discomfort indices will degenerate as a function of *disturbance prediction error*.

The rest of the paper is organized as follows. Section 2 presents the proposed high-level thermal model for buildings. We present the system dynamics used in the control derivation problem along with the state and input constraints and the uncertain model in Section 3. Section 4 describes the robust control strategies exploited in the paper. Section 5 presents the indices based on which we assess the performances of the introduced controllers. Section 6 presents results obtained from simulation of controllers and a comparison of their performance for different uncertainty bounds. Conclusions are drawn in Section 7.

2 Building Thermal Model

We use the model that was proposed in [8] in which the building is considered as a network. There are two types of nodes in the network: walls and rooms. There are in total n nodes, m of which represent rooms and the remaining $n-m$ nodes represent walls. The temperature of the i-th wall is governed by the following equation:

$$C_{w_i}\frac{dT_{w_i}}{dt} = \sum_{j\in\mathcal{N}_{w_i}} \frac{T_j - T_{w_i}}{R'_{ij}} + r_i\alpha_i A_i q''_{rad_i} \tag{1}$$

where T_{w_i}, C_{w_i}, α_i and A_i are the temperature, heat capacity, absorption coefficient and area of wall i, respectively. R'_{ij} is the total resistance between wall i and node j. q''_{rad_i} is the radiative heat flux density on wall i. $\mathcal{N}_{w_i}$ is the set of all of neighboring nodes to node w_i and, r_i is equal to 0 for internal walls, and to 1 for peripheral walls.

The temperature of the i-th room is governed by the following equation:

$$\begin{aligned} C_{r_i}\frac{dT_{r_i}}{dt} = &\sum_{j\in\mathcal{N}_{r_i}} \frac{T_j - T_{r_i}}{R'_{ij}} + \dot{m}_{r_i}c_a(T_{s_i} - T_{r_i}) \\ &+ w_i\tau_{w_i}A_{w_i}q''_{rad_i} + \dot{q}_{int_i} \end{aligned} \tag{2}$$

where T_{r_i}, C_{r_i} and $\dot{m}_{r_i}$ are the temperature, heat capacity and air mass flow into the room i, respectively. c_a is the specific heat capacity of air, A_{w_i} is the total area of window on the walls surrounding room i, τ_{w_i} is the transmissivity of glass of window i, q''_{rad_i} is the radiative heat flux density radiated to node i and $\dot{q}_{int_i}$ is the internal heat generation in thermal zone i. $\mathcal{N}_{r_i}$ is the set of all of the neighboring nodes to room i and, w_i is equal to 0 if none of the walls surrounding room i has window, and is equal to 1 if at least one of them has. The details of building thermal modeling and estimation of the un-modeled dynamics is presented by the authors in [2, 7, 8].

The heat transfer equations for each wall and room in the building yields the following state space form of the system dynamics

$$\begin{aligned} \dot{x}_t &= Ax_t + f(x_t, u_t, d_t) \\ y_t &= Cx_t \end{aligned} \tag{3}$$

where $x_t \in \mathbb{R}^n$ is the state vector representing the temperature of the nodes in the thermal network, $u_t \in \mathbb{R}^{l.m}$ is the input vector representing the air mass flow rate and discharge air temperature of conditioned air into each thermal zone, and $y_t \in \mathbb{R}^m$ is the output vector of the system which represents the temperature of the thermal zones. l is the number of inputs to each thermal zone (e.g., air mass flow and supply air temperature). d_t is the vector of unmodeled dynamics which is a function of q''_{rad_i}, T_{out} and $\dot{q}_{int_i}$, and A and C are matrices of proper dimensions.

2.1 Internal and external disturbance loads

Heat flux is radiated from the sun to the exposed walls and to the peripheral rooms through windows. This heat flux is a function of the *altitude* and *azimuth* angle of the location of the building on the Earth, orientation of the considered wall or window, day of the year, time of the day, outside weather and sky condition, and etc., which makes it very hard to estimate the exact value of this quantity. The authors propose a methodology in [2] for estimating the unmodeled dynamics of the nonlinear system of the building. Unmodeled dynamics vector comprises the effect of the external heat loads from solar radiation and ambient air temperature as well as the internal heat gains from occupants and equipments using a parameterization technique, using two quantities, being the *ambient air temperature* and CO_2 *sensor measurement data*. However, due to *prediction errors* associated to imperfect weather predictions, random occupancy of the building and random internal loads, it is in general very hard to *accurately* predict the un-modeled dynamics of the system.

These disturbance loads are random; however by studying the historical data of a building for different seasons with distinctive weather conditions and various occupancy patterns, it is possible to find out the cumulative effect of the disturbance loads within a range of uncertainties, for any given weather condition and occupancy pattern, using similar techniques as the one proposed in [2]. For the rest of the paper we assume that the l_∞

Copyright © 2012 by ASME

norm[2] of the disturbance load to the building is known. Note that l_∞ norm of the disturbance load represents the maximum value of disturbance load during a given day, hence a good measure of worst-case scenario.

2.2 Testbed for model validation

We validate the model that was developed as discussed above using the historical data of zone temperature of a specific thermal zone at Bancroft library of UC Berkeley campus. The details of the model validation technique and its results can be found in [2, 8]. We use Air Mass Flow (AMF), Discharge Air Temperature (DAT), and Outside Air Temperature (OAT) data to simulate the thermal behavior of the considered zone, and compare the simulation results with the measured temperature data of the zone. WebCTRL of Automated Logic Corporation (ALC) is used to access the data.

The Existing Control Strategy (ECS) of the considered building is used as a basis to assess the effectiveness of the presented controllers. The ECS in this case, turns on the air flow valves at *5:00 am* and turns them off at *5:00 pm*. It is shown in [2] that this is a relatively conservative and energy-hungry control strategy which neglects the effects of outside weather condition and the building occupancy.

3 Preliminaries

3.1 System dynamics

We use the nonlinear system described in Section 2 and expressed in (3). The system dynamics is linearized around the nearest equilibrium point to the specified operating point of the system (details in [7]). The algorithm to find the equilibrium point of the system starts from an initial point and searches, using a *Sequential Quadratic Programming (SQP) algorithm*, until it finds the nearest equilibrium point. First we linearize the model considering all the inputs to the model. Once the system dynamics is linearized, we divide the inputs into *manipulated variables* and *disturbance variables*. Discretizing the state space realization leads to the following discrete time LTI system:

$$x_{k+1} = Ax_k + Bu_k + Ed_k \tag{4}$$

where $d_k \in \mathbb{R}^r$ stores the disturbance at time k and the original B obtained from linearization process is split into two parts $B^{'} = [B \;\; E]$. Where B stores the columns corresponding to the *manipulated variables* and E stores the columns of $B^{'}$ corresponding to the *disturbance variables*. In this study, air mass flow is a *manipulated variable* and we regard the rest of the inputs as *disturbance variables* as they are not controlled.

[2]For vector $x = (x_1, x_2, ..., x_n)$, the l_∞ norm is given by: $||x||_\infty := max(|x_1|, |x_2|, ..., |x_n|)$.

3.2 State and input constraints

The system is subject to input constraints

$$\mathcal{U} := \{u \in \mathbb{R}^m | S^u u \leq s^u\} \tag{5}$$

where $S^u \in \mathbb{R}^{q \times l.m}$, $s^u \in \mathbb{R}^q$ and $\mathcal{U} \subset \mathbb{R}^{l.m}$ is a bounded polytopic set. The polytopic constraints on the state is given by

$$\mathcal{X} := \{x \in \mathbb{R}^n | S^x x \leq s^x\} \tag{6}$$

where $S^x \in \mathbb{R}^{p \times n}$, $s^x \in \mathbb{R}^p$ and $\mathcal{X} \subset \mathbb{R}^n$.

3.3 Additive uncertainty

Consider the uncertain linearized system dynamics given by

$$x_{k+1} = Ax_k + Bu_k + E(d_k + w_k) \tag{7}$$

where the disturbance uncertainty $w_k \in \mathbb{R}^r$ is a stochastic disturbance. We assume it is only known to be bounded in some measure, but otherwise unknown. The set of possible disturbance uncertainties is denoted by $\mathcal{W}$ and $w_k \in \mathcal{W} \quad \forall k = 0, 1, ..., N-1$. The disturbance set $\mathcal{W}$ is one of the ingredients that determine the type of optimization problem we end up with. For an uncertain *Linear Programming* (LP) when the corresponding uncertainty set $\mathcal{W}$ is a polyhedron, then the robust counterpart is also an LP. When $\mathcal{W}$ is ellipsoidal, then the robust counterpart becomes a *second-Order Cone Programming* (SOCP) [15]. For this application we consider box-constrained disturbance uncertainties given by

$$\mathcal{W}_\lambda = \{w : ||w||_\infty \leq \lambda\} \tag{8}$$

As an example, Fig. 1 depicts the temperature of the room from the validated model and the corresponding estimated unmodeled dynamics (in dashed red). The additive uncertainty to the system yields a temperature trajectory which is shown in the same figure (in solid blue).

3.4 Disturbance prediction error

To illuminate the effectiveness of the controllers laid out in Section 4, we assess their performances for different *disturbance prediction error* values denoted by δ and defined as

$$\delta = \frac{\lambda}{||\mathbf{d}||_\infty} \tag{9}$$

Copyright © 2012 by ASME

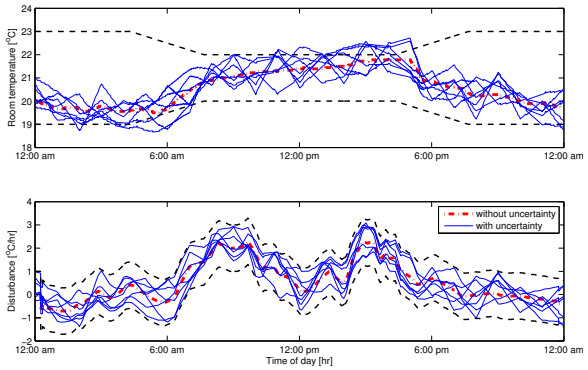

Figure 1. Room temperature and the corresponding unmodeled dynamics realization (in dashed red). Disturbance plus uncertainty and the corresponding room temperature for $\lambda = 1$ in the case of ECS is shown in solid blue. Note that although ECS is a rather conservative control strategy, it still fails to keep the temperature within the comfort zone at all times.

where λ is the l_∞ norm bound of the uncertainty and $\mathbf{d} = [d_1', d_2', ..., d_N']'$ is the disturbance realization vector[3].

3.5 Chance constraints

In this work we focus on uncertainty models given by (8). The results of this work can be easily extended to robust MPC problems with chance constraints such as [3]. Note that the uncertainty model used in [3] assumes independent and identically normally distributed random variables, i.e. $v \sim \mathcal{N}(0, I)$. However, the normally distributed disturbance v is approximated with a norm-bounded disturbance $w \in \mathbb{R}^p$, motivated with a work by the authors of [15] in which they show that a chance constraint of the form

$$\mathcal{X}_c = \{\mathbf{P}(\phi(x_0, U, \mathbf{d}, \mathbf{w}) \in \mathcal{X}) \geq 1 - \alpha\} \tag{10}$$

which requires that the condition $\phi(x_0, U, \mathbf{d}, \mathbf{w}) \in \mathcal{X}$ is fulfilled with a probability greater than or equal to $1 - \alpha$, can be approximated by a hard constraint if the uncertainty bound λ is chosen according to Theorem 5 in [3]. Note that $\phi(x_0, U, \mathbf{d}, \mathbf{w})$ denotes the solution to (7) given the initial state x_0, the control input $U = [u_1', u_2', ..., u_N']'$, the disturbance realization $\mathbf{d} = [d_1', d_2', ..., d_N']'$, and the uncertainty realization $\mathbf{w} = [w_1', w_2', ..., w_N']'$.

4 Controller design

As introduced in Section 3 we consider l_∞ bounded additive uncertainties in the control derivation.

[3]Note that x' represents the transpose of vector x.

4.1 Robust MPC against additive uncertainty

The crucial question in robust control is *how to exploit knowledge about uncertainty*. Typical knowledge can be bounds on uncertain parameters in the system, or bounds on external disturbances, such as the disturbance load to the building. In this paper we consider additive uncertainty to the system model as described in (7).

A typical robust strategy involves solving a min-max problem to optimize worst-case performance while enforcing input and state constraints for all possible disturbances. In this section we formulate a min-max robust constrained optimal control problem for the building air temperature regulation system affected by additive bounded input disturbances.

4.1.1 Open-Loop Predictions A min-max strategy for MPC tries to optimize the worst-case scenario cost function with respect to uncertainties. Define the worst-case cost function as

$$\begin{aligned} J_0(x(0), U_0) \triangleq \max_{w_{[.]}} \quad & \{||Px_N||_p + \sum_{k=0}^{N-1} ||Qx_k||_p + ||Ru_k||_p\} \\ \text{s.t.} \quad & x_{k+1} = Ax_k + Bu_k + E(d_k + w_k) \\ & w_k \in \mathcal{W} \\ & \forall \quad k = 0, \cdots, N-1 \end{aligned} \tag{11}$$

Where $||.||_p$ can be any polytopic norm and N is the time horizon. The robust optimal control problem is formulated as follows

$$J_0^*(x(t)) \triangleq \min_{U_t} \quad J_0(x(t), U_t) \tag{12}$$

subject to:

$$x_{k+1} = Ax_k + Bu_k + E(d_k + w_k) \qquad k = 0, \cdots, N-1 \tag{13a}$$
$$y_k = Cx_k \qquad k = 1, \cdots, N \tag{13b}$$
$$u_k \in \mathcal{U} \qquad k = 0, \cdots, N-1 \tag{13c}$$
$$x_k \in \mathcal{X} \qquad k = 1, \cdots, N \tag{13d}$$
$$\forall \ w_k \in \mathcal{W} \qquad k = 0, \cdots, N-1 \tag{13e}$$

At each time step t, only the first entry of U_t is implemented on the plant. At the next time step the prediction horizon N is shifted leading to a new optimization problem. This process is repeated until the total time span of interest is covered.

Using the above formulation, we derive a robust counterpart of an uncertain optimization problem in which constraints are satisfied for all possible uncertainties, and worst-case objective is

Copyright © 2012 by ASME

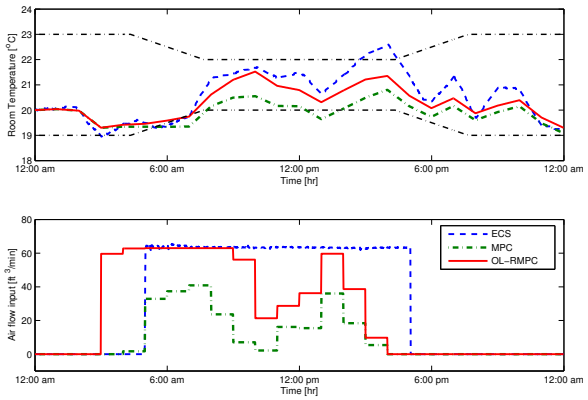

Figure 2. Performance of MPC and OL-RMPC in the presence of additive uncertainty with $\delta = 50\%$. It can be observed that the OL-RMPC yields an overly conservative control algorithm resulting in excessive energy consumption.

calculated. This system does not involve the uncertain variables anymore, and corresponds to the worst-case scenario model.

Performances of MPC and OL-RMPC are depicted in Fig 2. In the case of MPC, the controller is designed for the model with only disturbance d_k known a priori, and implemented on the model which has as input, both known disturbance d_k and the unknown additive uncertainty w_k.

4.2 Approximate closed-loop min-max MPC

It is shown in Fig. 2 that the Open Loop Constrained Robust Optimal Control (OL-CROC) is conservative. This is because we are optimizing an open-loop control sequence that has to cope with all possible future disturbance realizations, without taking future measurements into account. The Closed-Loop Constrained Robust Optimal Control (CL-CROC) formulation overcomes this issue but it can quickly lead to an intractable problem [13]. There are some alternative approaches which introduce feedback in the system and, in some cases, can be more efficient than CL-CROC.

4.2.1 Feedback predictions What we really would like to solve is the closed-loop min-max problem where we incorporate the notion that measurements will be obtained in the future times.

$$\min_{u_{k|k}} \max_{w_{k|k}} \cdots \min_{u_{k+N-1|k}} \max_{w_{k+N-1|k}} \sum_{j=0}^{N-1} p(x_{k+j|k}, u_{k+j|k}) \qquad (14)$$

where $p(.)$ is the performance index. Instead of solving this intractable problem, the idea in feedback prediction, sometimes referred to as closed-loop predictions, is to introduce new decision variables $v_{k+j|k}$, and parameterize the future control sequences in the future states and $v_{k+j|k}$ such as $u_{k+j|k} = m_{k,j}x_{k+j|k} + v_{k+j|k}$. This way, there is at least some kind of feedback in the system, although not optimal. To incorporate feedback predictions, we write the feedback predictions in a vectorized form $U = \mathbf{M}X + \mathbf{v}$. Where $\mathbf{v}$ and X are given by $\mathbf{v} = [v'_{k|k}, v'_{k+1|k}, \cdots, v'_{k+N-1|k}]'$, and $X = [x'_{k|k}, x'_{k+1|k}, \cdots, x'_{k+N-1|k}]'$. The only requirement for matrix $\mathbf{M}$ is that this matrix is *causal* in the sense that $u_{k+j|k}$ only depends on $x_{k+i|k}$, $i \leq j$. Notice that feedback predictions introduce a new tuning knob in min-max MPC, which is matrix $\mathbf{M}$. However the choice of $\mathbf{M}$ is not obvious, and no guideline exists in the literature, on how to select its entries. In [13] it is shown through simulation examples that the choice of $\mathbf{M}$ is crucial for good performance of the min-max controller.

However sometimes $\mathbf{M}$ is incorporated as a decision variable in the online optimization problem. The obtained optimization problems are convex. Unfortunately, the optimization problem grows rapidly, although polynomially in the system dimension, the number of constraints and the prediction horizon. To resolve this problem, it is shown in [13] how the general solution can serve as a basis for off-line calculations, and approximations with a reduced degree of freedom, but with much better computational properties (we have somehow implemented this idea in constructing a better $\mathbf{M}$ in what follows).

The main problem with the min-max formulations based on these parameterizations is the excessive number of decision variables and constraints. The reason is the high-dimensional parameterization of matrix $\mathbf{M}$.

4.2.2 Alternative Parameterizations To resolve this issue we study some other parameterizations that have been introduced in the literature and also the parameterization that we introduce later in this paper.

It is shown in [13] that the problem with the parameterization introduced previously, is that the mapping from $\mathbf{M}$ and $\mathbf{v}$ to X and U is nonlinear, hence optimization over both $\mathbf{M}$ and $\mathbf{v}$ is likely to cause problem. At least, it is not obvious how this parameterization can be incorporated in a standard convex optimization framework. Due to this problem, alternative parameterizations are introduced. One of the parameterizations introduced in [13] is as follows:

1. Lower Triangular Structure (LTS): Define the affine disturbance feedback as:

$$u_i := \sum_{j=0}^{i-1} m_{i,j}w_j + v_i \qquad \forall i = 1,2,...,N-1 \qquad (15)$$

where $M_{i,j} \in \mathbb{R}^{l.m \times r}$ and $v_i \in \mathbb{R}^{l.m}$ are given by

Copyright © 2012 by ASME

$$\mathbf{M} := \begin{bmatrix} 0 & \cdots & \cdots & 0 \\ m_{1,0} & 0 & \ddots & 0 \\ \vdots & \ddots & \ddots & \vdots \\ m_{N-1,0} & \cdots & m_{N-1,N-2} & 0 \end{bmatrix}, \quad \mathbf{v} := \begin{bmatrix} v_0 \\ \vdots \\ \vdots \\ v_{N-1} \end{bmatrix} \tag{16}$$

and $\mathbf{w} = [w_0 \quad w_1 \quad \cdots \quad w_{N-1}]'$ is the vector of disturbance. Therefore the input can be written as $U = \mathbf{M}\mathbf{w} + \mathbf{v}$. The control sequence is now parameterized directly in the uncertainty. The mapping from $\mathbf{M}$ and $\mathbf{v}$ to X and U is now bilinear. What we have here is basically a sub-optimal version of the closed-loop min-max solution [13].

Note that other parameterizations such as *Toeplitz* are also introduced in [13]. However, Toeplitz structure was shown to deteriorate the performance of the CL-RMPC in our simulations and therefore is not considered here.

2. Two Lower Diagonal Structure (TLDS): By analyzing the structure of the optimal matrix $\mathbf{M}$, we observed that the parameterization of the input need not consider feedback of more than past two values of $\mathbf{w}$ at each time, hence we propose the following disturbance feedback:

$$\begin{aligned} u_i &:= m_{i,i-2}w_{i-2} + m_{i,i-1}w_{i-1} + v_i \\ &= \sum_{j=i-2}^{i-1} m_{i,j}\omega_j + v_i \qquad \forall i = 1,2,...,N-1 \end{aligned} \tag{17}$$

and the corresponding parameterization matrix $\mathbf{M}$ is an $N \times N$ matrix that has the entries on the first and second diagonal of $\mathbf{M}$ below its main diagonal as decision variables and 0 elsewhere as given by

$$\mathbf{M} = \begin{bmatrix} 0 & 0 & \cdots & 0 & 0 & 0 \\ m_{21} & 0 & 0 & \cdots & 0 & 0 \\ m_{31} & m_{32} & \ddots & \vdots & \vdots & \vdots \\ 0 & m_{42} & \ddots & 0 & \vdots & \vdots \\ \vdots & \ddots & \ddots & m_{1,2} & 0 & 0 \\ 0 & \cdots & 0 & m_{N,N-2} & m_{N,N-1} & 0 \end{bmatrix} \tag{18}$$

and $\mathbf{v}$ remains as in the previous structure. Note that in this structure we exploit the sparsity of the feedback gain matrix to enhance the computational characteristics of the optimal problem.

A schematic of the robust optimal control implementation on the nonlinear building model is depicted in Fig. 3.

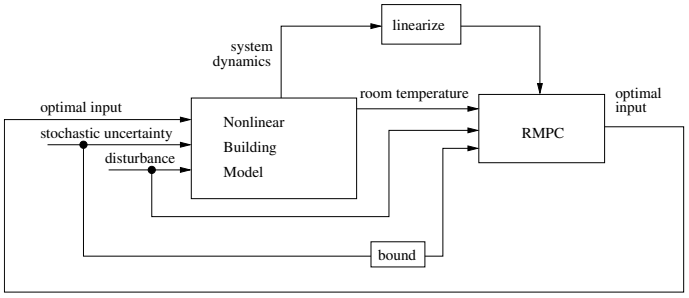

Figure 3. Schematic of the control implementation.

5 Performance Indices

To compare the overall performance of the proposed controllers we define two indices to measure the energy consumption and comfort level provided by each controller.

The energy index I_e, is defined to be

$$I_e = \int_{t=0}^{24} [P_c(t) + P_h(t) + P_f(t)]\, dt \tag{19}$$

where cooling power P_c, heating power P_h and fan power P_f are defined as

$$P_c(t) = \dot{m}_c(t) c_p [T_{out}(t) - T_c(t)] \tag{20}$$

$$P_h(t) = \dot{m}_h(t) c_p [T_h(t) - T_{out}(t)] \tag{21}$$

$$P_f(t) = \alpha \dot{m}^3(t) \tag{22}$$

where $c_p = 1.012[kJ/kg.^oC]$ is the specific heat capacity of air and $\alpha = 0.5[kW.s^3/kg^3]$ is the fan power constant. Using the above equations and constants, results in fan power values in $[kW]$.

The discomfort index I_d, is defined as the sum of all the temperature violations during the course of a day.

$$I_d = \int_{t=0}^{24} \left[\min \left\{ \left| T(t) - \overline{T}(t) \right|, \left| T(t) - \underline{T}(t) \right| \right\} . \mathbf{1}_{\mathcal{B}(t)^c}(T(t)) \right] dt \tag{23}$$

Where $\mathcal{B}(t) = [\underline{T}(t), \overline{T}(t)]$ is the allowable temperature boundary at time t and $\mathbf{1}$ is the indicator function.

6 Simulation results

We implement the introduced controllers with a prediction horizon of $N = 24$. We observed a dramatic degradation of the performance for $N < 24$, and relatively long computational time for $N > 24$. We believe the choice of $N = 24$ leads to a good balance between performance and computational cost. The utilized cost function for the following simulations is given by

Copyright © 2012 by ASME

$$\min_{U_t,\bar{\varepsilon},\underline{\varepsilon}} \quad \{||\mathbf{U_t}||_1 + c_1||\mathbf{U_t}||_\infty + c_2(||\overline{\varepsilon}_\mathbf{t}||_1 + ||\underline{\varepsilon}_\mathbf{t}||_1)\} \tag{24}$$

and the state and input constraints are as follows:

$$x_{t+k+1|t} = Ax_{t+k|t} + Bu_{t+k|t} + E(d_{t+k|t} + w_{t+k|t}) \tag{25a}$$
$$y_{t+k|t} = Cx_{t+k|t} \tag{25b}$$
$$\underline{T}_{t+k|t} - \underline{\varepsilon}_{t+k|t} \leq y_{t+k|t} \leq \overline{T}_{t+k|t} + \overline{\varepsilon}_{t+k|t} \tag{25c}$$
$$u_{t+k|t} \leq \overline{u} \tag{25d}$$
$$\underline{\varepsilon}_{t+k|t},\ \overline{\varepsilon}_{t+k|t} \geq 0 \tag{25e}$$
$$w_{t+k|t} \in \mathcal{W} \tag{25f}$$

where $\overline{u} = 63\ \ [ft^3/min]$ is the higher limit on air mass flow, $[\underline{T}_{.|t}\ \ \overline{T}_{.|t}] = [20\ \ 22]^oC$ during occupied hours and $[\underline{T}_{.|t}\ \ \overline{T}_{.|t}] = [19\ \ 23]^oC$ during unoccupied hours. We utilize soft constraints to guarantee feasibility of the problem at all time steps. For the simulations we use $c_1 = 0.75$ and $c_2 = 50$.

The optimal controller and the resulting room temperature with the presence of a box-constrained uncertainty in four cases is depicted in Fig. 4. ECS refers to the Existing Control Strategy implemented on the building. This case shows the behavior of the original controller of the building if there were a hypothetical extra additive load to the system. The next case shows the performance of an MPC algorithm with only the accurate a priori knowledge of the disturbance (i.e. unmodeled dynamics of the system) and not the uncertainty. The third case is OL-RMPC in which the algorithm has a priori knowledge of both the disturbance and the uncertainty bound. The fourth case algorithm is a CL-RMPC which exploits the same knowledge as the third case, with the difference that it utilizes the uncertainty feedback strategy of (15).

We consider stochastic uncertainties with different uncertainty bounds (λ) as introduced in (8). The MPC does not have any a priori information regarding the additive uncertainty, and calculates the controller solely based on the deterministic system dynamics. However the RMPC integrates the uncertainty bound information in the control derivation. Controller performances are evaluated based on the energy and discomfort indices introduced in Section 5.

Remark 1. It can be observed from Fig. 4, that the OL-RMPC and CL-RMPC are the only two controllers that are able to keep the temperature within the comfort zone, at all times, with the difference that the CL-RMPC leads to 36% reduction in energy index, I_e, while maintaining perfect level of comfort ($I_d = 0$).

Fig. 5 depicts how *Discomfort index* I_d, varies with disturbance prediction error δ for MPC, OL-RMPC and CL-RMPC. It is shown that both OL-RMPC and CL-RMPC manage to keep the perfect comfort level ($I_d = 0$), for prediction errors up to

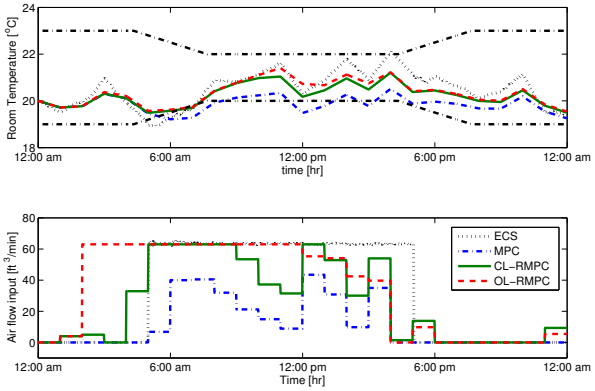

Figure 4. Control input and resulting temperature profile for original controller, open-loop, closed-loop and regular MPC. The additive uncertainty bound is considered $\delta = 60\%$ in this case.

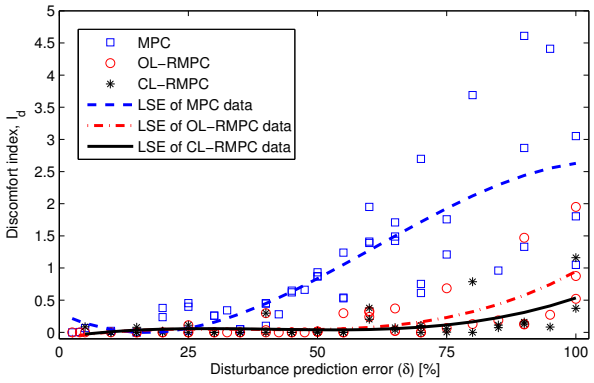

Figure 5. Discomfort index I_d $[^oCh]$ versus disturbance prediction error (δ). We generate a uniform random sequence based on the disturbance prediction error value δ. The generated random sequence is used in the simulations for making this graph. Note that different data points for one δ value refers to simulations with different random sequences. The reason for such wide deviation of the simulation results stems from the fact that depending on the value of the random variable at any time, the resulting disturbance vector can either lead to higher or lower temperature deviations with respect to the nominal disturbance value. Note that LSE refers to Least Square Estimation.

$\delta = 60\%$ and $\delta = 75\%$ respectively, while the MPC maintains the perfect comfort level for uncertainty bounds up to $\delta = 20\%$. The discomfort index for MPC goes as high as 4.61 $[^oCh]$[4] while the value for CL-RMPC reaches 1.2 $[^oCh]$ in the worst case in the simulations corresponding to $\delta = 100\%$.

Fig. 6 depicts the variations of *Energy index* I_e, versus the uncertainty bound on the unmodeled dynamics. It is clear that the energy index for RMPC increases dramatically with δ, while the energy index for MPC changes slightly. However, this comes

[4] degree Celsius hour.

Copyright © 2012 by ASME

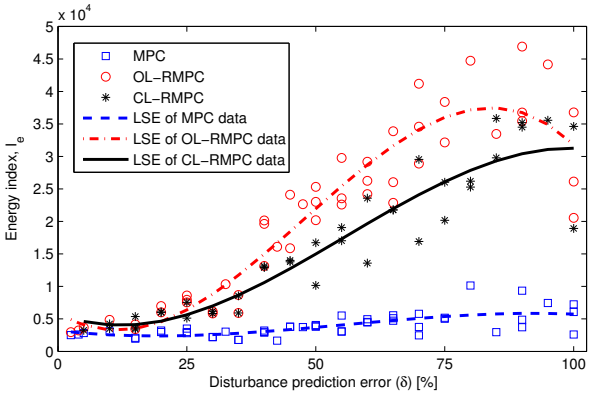

Figure 6. Energy index I_e $[kWh]$ versus disturbance prediction error (δ). The data points for this graph were generated using a similar technique as in Figure 5. Note that LSE refers to Least Square Estimation.

with the drawback of increased discomfort index for MPC.

Remark 2. Exploiting the *TLDS* structure results in the same control law that was obtained from the *LTS* structure. Matrix $\mathbf{M}$ of *LTS* has $l.m.r\frac{N(N-1)}{2}$ variables (quadratic in N) while matrix $\mathbf{M}$ of *TLDS* has $l.m.r(2N-3)$ variables (linear in N), and hence exhibits faster computation characteristics. On average, the simulation time for *TLDS* is 30% less than the *LTS* structure, as shown in Table 1.

The problem is solved using CPLEX 12.2 [16] on a 2.67 GHz machine with 4 GB RAM. We observed about 33% reduction in the simulation time, in average, when we used CPLEX compared to the default solver of YALMIP [17], GLPK.

An important point to notice from Fig. 6 is how much more energy needs to be supplied to the HVAC system to maintain the comfort level in the presence of imperfect and faulty unmodeled dynamics predictions. Consider the case where $\delta = 75\%$. MPC will lead to a discomfort index of 1.7^oCh on average, while the RMPC is able to maintain the temperature below a discomfort index of 0.016^oCh on average. However this level of comfort provided by the CL-RMPC comes at a cost of energy consumption of almost 5 times more than the MPC case.

Remark 3. Note that due to the tradeoff between comfort and energy consumption, the choice of which controller to use is on the building HVAC operator, and depends on various factors such as criticality of meeting the temperature constraints for the considered thermal zone in the building, and availability and price of energy at that time of the day/year.

As observed from Fig. 5 and 6 the behavior of controllers deviate considerably as the prediction error increases. For instance, The energy required to keep the same level of comfort for CL-RMPC in the case of $\delta = 75\%$ is almost 4 times the energy required to provide the same level of comfort when $\delta = 25\%$. Therefore, these two plots make it clear how precious a good model which *accurately* captures also the unmodeled dynamics of the system can be in minimizing the operation costs of HVAC systems of buildings.

Table 1. Comparison of LTS and TLDS uncertainty feedback parameterizations and Open Loop min-max results for the case of $\delta = 50\%$.

Controller	Number of feedback decision variables	Average simulation time for $N = 24$, in [s]	I_e $[kWh]$	I_d $[^oCh]$
LTS	$l.m.r(\frac{N(N+1)}{2})$	200	16467	0
TLDS	$3l.m.r(N-1)$	138	16467	0
OL	-	159	22592	0.84

7 Conclusion

We presented a model predictive control strategy that is robust against additive uncertainty. Uncertainties are introduced to the building thermal model through imperfect weather and occupancy predictions. We study the performance of two robust optimal control strategies, i.e. Open-Loop Robust Model Predictive Control (OL-RMPC) and Closed-Loop Robust Model Predictive Control (CL-RMPC) on a building model. CL-RMPC is capable of maintaining the temperature within the comfort zone for disturbance prediction errors up to $\delta = 75\%$ as opposed to nominal MPC which can maintain the perfect comfort level for prediction errors up to $\delta = 20\%$. The open-loop and closed-loop strategies studied here exhibit similar performances in terms of constraint satisfaction with CL-RMPC *outperforming* at higher disturbance prediction error values. The CL-RMPC strategy also outperforms the OL-RMPC strategy in terms of energy consumption, leading to maximum of 36% reduction in *energy index* at $\delta = 75\%$ while resulting in an even lower discomfort index than the OL-RMPC case.

We proposed a new uncertainty feedback parameterization of the control input, *TLDS*, for the CL-RMPC which results in the same energy and discomfort indices as the previous parameterization, *LTS*, with a lower number of decision variables, *linear* in time horizon N, as opposed to *quadratic*, for the *LTS* as shown in Table 1. The new *TLDS* parameterization results in an average simulation time of 30% less than *LTS*.

REFERENCES

[1] A. Standard, "90.1-1989," *American Society of Heating, Refrigerating, and Air-Conditioning Engineers*, 1989.

[2] M. Maasoumy and A. Sangiovanni-Vincentelli, "Total and peak energy consumption minimization of building hvac systems using model predictive control," *IEEE Design and Test of Computers*, Jul-Aug 2012.

[3] F. Oldewurtel, C. Jones, and M. Morari, "A tractable approximation of chance constrained stochastic mpc based on affine disturbance feedback," in *Decision and Control, 2008. CDC 2008. 47th IEEE Conference on*, pp. 4731–4736, IEEE, 2008.

Copyright © 2012 by ASME

[4] A. D. Y. Ma, A. Kelman and F. Borrelli, "Model predictive control of thermal energy storage in building cooling systems," *IEEE Control System Magzine*, pp. 1–65, 2011.

[5] Y. Ma, F. Borrelli, B. Hencey, B. Coffey, S. Bengea, and P. Haves, "Model predictive control for the operation of building cooling systems," in *American Control Conference (ACC), 2010*, pp. 5106–5111, IEEE, 2010.

[6] F. Oldewurtel, A. Parisio, C. Jones, M. Morari, D. Gyalistras, M. Gwerder, V. Stauch, B. Lehmann, and K. Wirth, "Energy efficient building climate control using stochastic model predictive control and weather predictions," in *American Control Conference (ACC), 2010*, pp. 5100–5105, IEEE, 2010.

[7] M. Maasoumy Haghighi, "Modeling and optimal control algorithm design for hvac systems in energy efficient buildings," Master's thesis, EECS Department, University of California, Berkeley, Feb 2011.

[8] M. Maasoumy, A. Pinto, and A. Sangiovanni-Vincenteli, "Model-based hierarchical optimal control design for HVAC systems," in *Dynamic System Control Conference (DSCC), 2011*, ASME, 2011.

[9] K. Deng, P. Barooah, P. Mehta, and S. Meyn, "Building thermal model reduction via aggregation of states," in *American Control Conference (ACC), 2010*, pp. 5118–5123, IEEE, 2010.

[10] J. Rossiter, *Model-based predictive control: a practical approach*. CRC, 2003.

[11] F. Borrelli, A. Bemporad, and M. Morari, "Predictive control for linear and hybrid systems." to be published, Apr. 2011.

[12] J. Lofberg, "Approximations of closed-loop minimax mpc," in *Decision and Control, 2003. Proceedings. 42nd IEEE Conference on*, vol. 2, pp. 1438–1442, IEEE, 2003.

[13] J. Löfberg, *Minimax approaches to robust model predictive control*. Univ., 2003.

[14] A. Bemporad and M. Morari, "Robust model predictive control: A survey," *Robustness in identification and control*, pp. 207–226, 1999.

[15] D. Bertsimas and M. Sim, "Tractable approximations to robust conic optimization problems," *Mathematical Programming*, vol. 107, no. 1, pp. 5–36, 2006.

[16] "Ibm ilog cplex optimizer," Feb. 2012.

[17] J. Löfberg, "Yalmip : A toolbox for modeling and optimization in MATLAB," in *Proceedings of the CACSD Conference*, (Taipei, Taiwan), 2004.

Copyright © 2012 by ASME